htw saar

Systems Neuroscience
& Neurotechnology Unit

Closed Loop Virtual Reality for the Treatment of Phobias

Bachelor Thesis

Systems Neuroscience & Neurotechnology Unit
Saarland University of Applied Sciences
Faculty of Engineering

Submitted by	:	Dominik Limbach
Matriculation Number	:	3662306
Course of Study	:	Biomedical Engineering (Bachelor)
First Supervisor	:	Prof. Dr. Dr. Daniel J. Strauss
Second Supervisor	:	Dr. Lars Haab

Saarbrücken, March 5, 2018

Declaration

I hereby declare that I have authored this work independently, that I have not used other than the declared sources and resources, and that I have explicitly marked all material which has been quoted either literally or by content from the used sources. This work has neither been submitted to any audit institution nor been published in its current form.

Saarbrücken, March 5, 2018

Dominik Limbach

Abstract

we want to find out if it is possible to design a fully automatic therapy system using vr and psycho physiological measurement. therefor we will test our virtual environment with a random group of subjects and measure ecg and gsr the goal of the conducted experiment is to show that our virtual reality is capable ob causing fear this will be done by evaluating the measured bio data

furthermore our virtual can be controlled by a therapist the therapist will be able to exercise control through a matlab program provided with real time visual data the therapist will be a substitute for the AI which will later be controlling the vr respectively to the measured data

the vr and the related pc will feed visual input to the subject this input is processed by the subject and he gives output information in the form of gsr and heart rate serving as input for our third system, the therapist (visual presentation of processed data) therapist can control vr —loop closed

Zusammenfassung

translation of abstract

Acknowledgments

Contents

1 Introduction

Virtual reality combines real-time computer graphics, body-tracking devices and high-resolution visual displays to create a computer-generated virtual environment. With their ability to immerse the user into a virtual mirror of the real world, virtual environments are a powerful tool in clinical application, especially in the treatment of phobias (Riva, 2003).
Studies have shown anxiety disorders to be the most prevalent mental disorders (Kessler et al., 2005). Many consider exposure therapy the most effective form of treatment for specific phobias (DeRubeis and Crits-Cristoph,1998). However that may be, considering the nature of certain phobias such as fear of heights, exposure therapy involves a genuine risk of injury. Performing therapy in a virtual environment therefore can be a promising alternative to the conventional in-vivo exposure.
The efficacy of virtual reality exposure therapy (VRET) has already been demonstrated in the past. A study conducted on acrophobia compared two groups of student subjects. The first group received a graded VRET. Students of the second group were added to a waiting-list as a control group. Results showed that VRET is more effective than no treatment (Rothbaum et al.,1995). VRET was also found to be as effective as exposure in-vivo in a more recent work by Emmelkamp et al. (2002).
In addition to this using a virtual reality system can have a number of advantages over in-vivo exposure. First and foremost being the ability to conduct therapy inside a controlled and secure environment like a therapist's office. This also implies therapy being less time consuming and provides considerable financial benefits (Cavanagh and Shapiro, 2004). The possibility of having therapy in a more private scenario also could lead to it becoming a more attractive choice for patients, that are too anxious or fear public embarrassment. A recent study exploring the acceptability of virtual reality exposure and in-vivo exposure in subjects suffering from specific phobias supports this hypothesis. Seventy-six percent chose virtual reality over in-vivo exposure. In addition to this the refusal rate of 3% for virtual reality exposure was substantially lower than 27% for in-vivo exposure (Garcia-Palacios et al., 2007). Further epidemiological studies show a lifetime prevalence of 28.5% for vHI and 6.4% for acrophobia alone and only 11% of susceptible people consulting a doctor (Huppert et al., 2013; Kapfhammer et al.,2015).
These results suggest that virtual reality exposure could help increase the number of people who seek therapy for phobias and therefore needs to be established in everyday clinical work.
In recent years there has been a lot of research on virtual reality treatment for different phobias trying just that.

For example a controlled study by Rothbaum et al. on aerophobia (2000) as well as a open clinical trial post-traumatic stress disorder (2001) and a study on agoraphobia (Meyerbröker et al.,2011), all of which yielded positive results. There also have been studies on ways to control the virtual reality. In a pilot study, Levy et al. (2015) explored the possibility of a remote-controlled virtual reality. After a trial session in a neutral virtual environment the patients received a total of six therapy sessions. The first three sessions were remote-controlled virtual reality exposure therapy (e-VRET) followed by three sessions in the presence of a therapist (p-VRET). E-VRET sessions were conducted without any contact to the hospital staff. The study showed that e-VRET not only is possible but produces results equal to p-VRET. Assessing the mental state of a patient is essential for the success of the therapy. A task which usually falls to the hands of the therapist and in most cases relies on a verbal communication between both parties. Past studies have shown a strong psychophysiological arousal in in-vivo exposure for different specific phobias (Nesse et al.,1985; Alpers and Sell,2007). In a more recent work Diemer et al. (2015) also confirmed physiological arousal in subjects executing a virtual height challenge. The study examined phobics and healthy controls in terms of subjective and physiological fear reactions resulting in a significant increase of subjective fear, heart rate and skin conductance level. To prove this hypothesis, we designed a virtual environment for the treatment of acrophobia that is sufficiently adaptable to various degrees of acrophobia. We will show the effectiveness of our system based on a subjective rating as well as heart rate and skin conductance measurements. Further we will deploy our virtual environment in a closed loop virtual reality system, featuring multiple control units. We will conduct a experiment simulating the effect of real-time physiology based decision making by using a remote-controlled virtual reality.

1.1 Theoretical Background

In this chapter, we will give a brief introduction to the field of anxiety disorders, especially specific phobias and the associated therapy concept, which is exposure therapy. The first part will contain fundamentals on phobias, exposure therapy and the concept of fear. Furthermore we will elaborate on the psychophysiological influences of stress and anxiety on certain parts of the human body and functions as well as methods of determination in physiological measurement. The second part will recapitulate recent approaches on virtual reality exposure therapy and analyze existing problems.

1.1.1 Acrophobia

1.1.2 Stress

1.1.3 Electrodermal Activity

Electrodermal activity (EDA) is a collective term for all electrical phenomena in the skin, which was first introduced by Johnson and Lubin (1966). This includes active and passive electrical properties, caused by skin functions and skin structure as well as the appendages of the skin.The skin appendages are structures formed by skin-derived cells such as hair, nails, sebaceous glands and sweat glands. EDA is one of the most commonly used response systems in psychophysiological research. This is due to its relative ease of measurement and its sensitivity to psychophysiological states and processes. The following section will provide a brief overview of EDA, ranging from physical and psychological context to recording and quantification methods.

Anatomical basis

This section will elaborate on the anatomical aspects of the human skin and will cover all the parts and appendages, that are needed to understand the principles of EDA. The skin or cutis is the biggest organ of the human body and inherits many different functions, which are essential for survival. It primarily acts as a selective barrier, preventing the entry of foreign matter and enables the passage of materials from the bloodstream to the exterior of the body. Other than protection, it is involved in thermoregulation, cutaneous circulation and immunologic protection. The anatomical structure of the skin is similar in most regions of the body. Although, specialized regions of skin, such as the palms and soles may be resembling in structure, they possess modified characteristics.

The human skin is composed of two clearly distinguishable layers, the epidermis that serves as a protective barrier and the dermis that provides nutrition. The cutaneous structures are vertically arranged and located on top of the subcutaneous tissue. Figure 1.1 shows a representation of each of the layers and their general spatial configuration among themselves.

The epidermis, on its own, can be divided into five different layers and lies on the surface of the skin. It consists of epithelial tissue, which is built in the lowest layer, the stratum germinativum. The main part of the produced cells are keratinocytes, which are able to store keratin and therefore become horny over time. The keratinocytes migrate to the surface of the skin, causing the epidermis to become more horny when approaching the surface. The outer layer is called the stratum corneum, originating from the fully

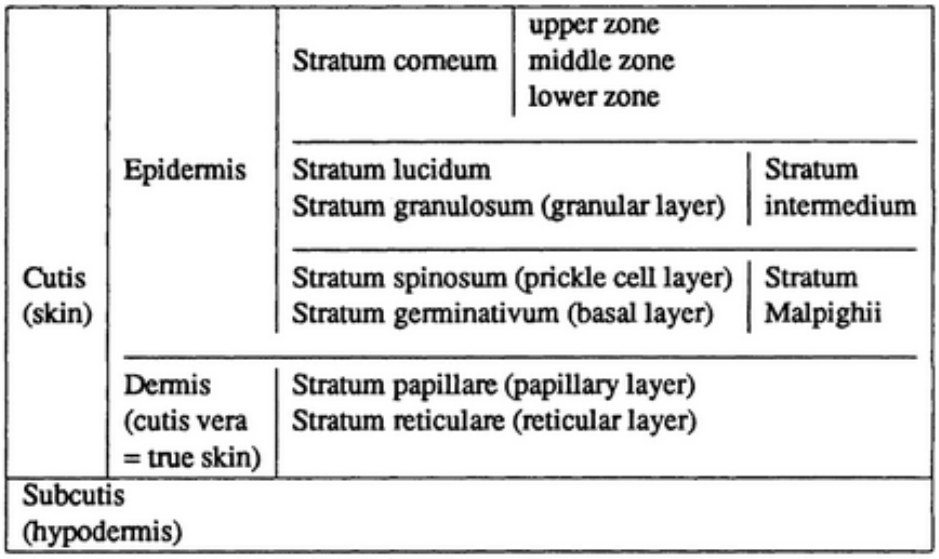

Figure 1.1: The Layers of the skin.The zonal layering is not so distinct in every skin region. Note that the stratum lucidum is only clearly recognizable on the palmar and plantar skin areas.[1]

keratinized state of its cells. On their way to the surface the keratinocytes undergo a number of specific changes in form and areal distribution, which in part are used to define the different epidermal layers. Also the cells become less tightly packed, compared to the deeper layers, causing the epidermis to become dryer towards the surface. A fact that greatly influences the electrical properties of the epidermis and therefore the electrodermal activity. The stratum corneum is especially thick in the palmar and plantar regions of the body. Reaching a thickness of approximately 1 mm, it is almost 20 times thicker than its overall average of 50 μm.
The dermis, which is also referred to as the corium, lies directly beneath the epidermis. Although it is much thicker than the epidermis it is only composed of two different dermal layers, the stratum papillare and the stratum reticulare, which are distinguishable by their density and the arrangement of their collagen fibers. The epidermal dermal junction, which is the transition area between the epidermis and dermis, resembles interlocking hands and is formed by a basal-membrane zone (Boucsein, 2013). The dermal layer, closest to the epidermis is called the papillary stratum. Other than the capillary net of arterial and venous blood vessels, it contains receptor organs as well as melanocytes and free collagen cells. The second dermal layer, which lies on top of the subcutaneous tissue, is called the reticular stratum. It wears this name because of its texture. Formed of strong collagenous fibers, reticular stratum is highly resistant to rupture, granting the dermis is leathery impression.

The subcutis, or hypodermis, is located beneath the dermis and is composed of loose connective tissue. It serves as a connection between the skin and the connective tissue of

the muscles, allowing for good horizontal mobility of the skin. The subcutis also serves as a thermal and mechanical insulation layer, due to its ability to store fat. In addition to this it, contains nerves and vessels, which supply the skin with nutrition and information, as well as the hair follicles and secretory part of the glands.

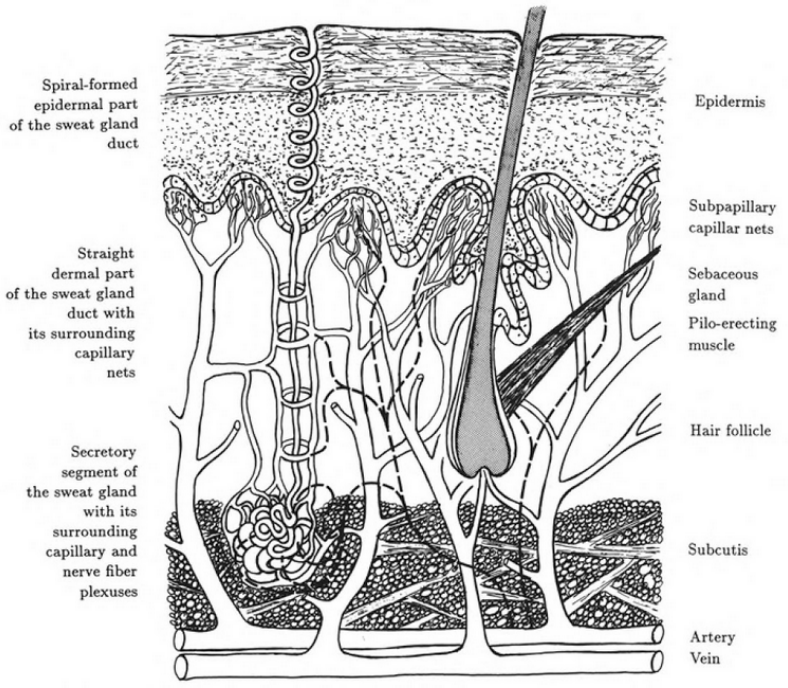

Figure 1.2: A artificial cross-section of the skin. It combines a sweat gland in ridged skin (left) and a hair together with a sebacous gland in polygonal skin (right).[1]

The left side of figure 1.2 shows an example for a typical profile of glabrous (hairless) skin. This specific form of skin differs in its horizontal structure. During early embryonal development specific patterns are formed by ridge formation. Ridged skin can be found on the palms of the hands and the soles of the feet. Areas, both of which, are frequently mechanically stressed and also have been found to have the highest densities of sweat glands, with an average of 233 sweat glands per cm^2 on the hands and 620 glands per cm^2 in adult's skin (Millington and Wilkinson 1983 in Boucsein, 2013). Sweat gland are considered to be exocrine glands, which is due to the fact that they secrete directly onto the surface of the skin. There are two types of human sweat glands, eccrine and apocrine, the majority being of the first type. The secretions of eccrine glands only contain negligible amounts of cytoplasm from the glandular cells. As there are no apocrine sweat glands located on the palmar skin, which is the most common location for EDA measurement, this section will only focus on eccrine sweat glands. The main purpose of eccrine sweat glands is to regulate the body temperature. With the exception of the palmar and plantar glands, which are thought to rather take part in grasping behavior (Edelberg, 1972, cited by Cacioppo et al., 2007). Further all eccrine sweat glands are believed to be more responsive to psychologically significant stimuli and therefore to

be involved in emotional sweating. Emotional sweating is primarily observable in areas with a high density of eccrine sweat glands, such as hands and feet. Therefore, making these region particularly interesting for EDA measurement, concerning the effect of psychophysiological stimuli. Before elaborating on the connection between electrodermal activity and sweat gland activity, it is useful to consider the anatomy of the glands first.

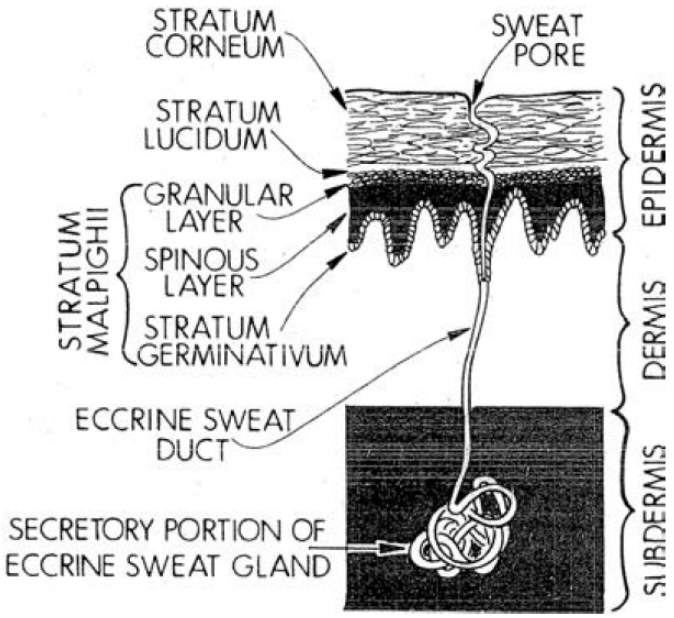

Figure 1.3: Anatomy of the eccrine sweat gland in various layers of glabrous skin.(Adapted from Hassett, 1978)[2]

Figure 1.3 shows the anatomy of an eccrine sweat gland in glabrous skin. It consists of the secretory portion, the coiled compact body of the gland, and the sweat duct. The sweat duct, which is the excretory portion of the gland, is a long tube reaching all the way to the stratum corneum, forming a small pore on the surface of the skin. It passes through the dermis in a relatively straight line but ends up spiraling through the epidermis (Edelberg, 1972, cited by Cacioppo et al., 2007). Imagining sweat glands as a set of variable resistors wired in parallel, helps to understand their influence on electrodermal activity. As sweat rises in the ducts their electrical resistance is constantly reduced, resulting in noticeable changes in electrodermal activity. The amount of sweat and the number of glands that are currently active, and therefore the electrodermal activity depends on the degree of activation of the sympathetic division of the autonomic nervous system.

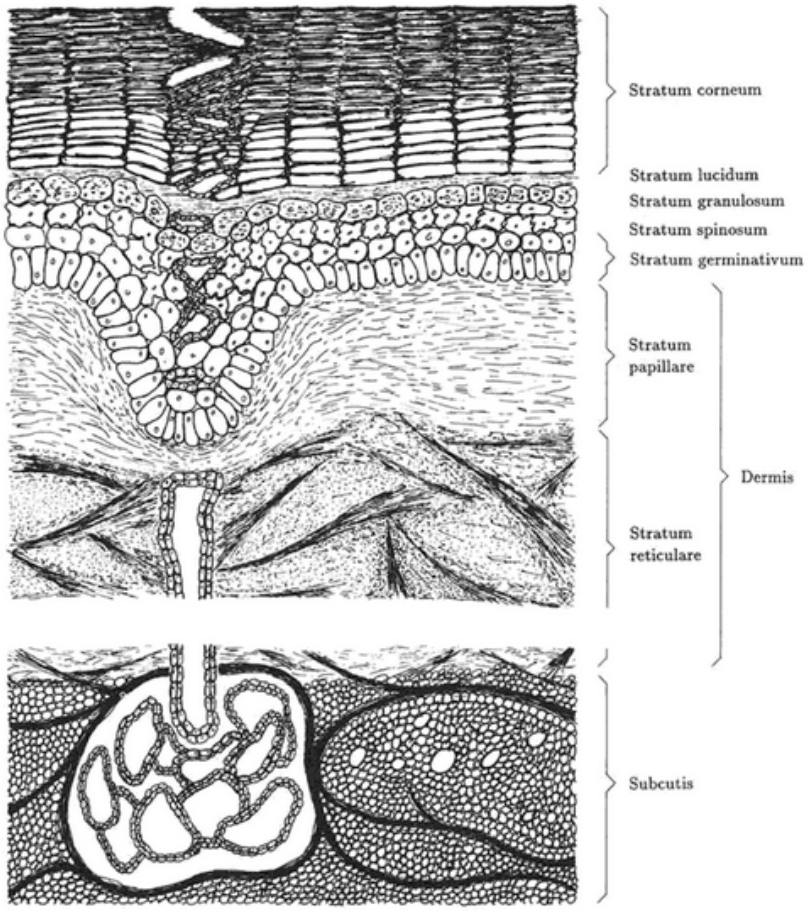

Figure 1.4: A cross-section of the layered construction of the glabrous human skin containing an eccrine sweat gland, in its glomerulus, together with its straight dermal and irregularly coiled epidermal duct. A part of the reticular layer has been omitted due to its size in relation to the rest. [1]

Physiological basis

According to the previous section, focusing on the anatomical aspects, this section will outline only the physiological mechanisms required to understand electrodermal mechanisms. The autonomic nervous system (ANS) is a complex systems of nerves that regulates involuntary and unconscious actions. The emphasis of this section will be its thermoregulatory aspects, which also involve the skin and sweat glands. There are a number of efferent vegetative fibers in the human skin, including sympathetic fibers, innervating the secretory segment of the eccrine sweat glands, and vasoconstrictive efferences for the blood vessels. Originating from the brain, the efferent sympathetic nerves descend in the anterolateral part of the spinal cord in close proximity to the pyramidal tract. They are switched over in the lateral horn and leave the spinal cord through its ventral root. Alongside motoric fibers, the preganglionic sympathetic fibers

travel via the white communicating ramus to the sympathetic trunk. From this point the neuronal activity will be distributed to various levels of the sympathetic trunk, causing one preganglionic fiber to reach up to 16 postganglionic neurons. The postganglionic fibers exit the sympathetic trunk through the gray communicating ramus and from there spread into the periphery, eventually reaching the skin.

Human sweat glands have predominantly sympathetic cholinergic innervation from sudomotor fibers originating in the sympathetic chain. The secretory part of the gland is surrounded by a dense plexus of sympathetic fibers. This allows for a wide distribution of ANS activity. The sudorisecretory fibers form a smooth bundle between the lateral pyramidal tract and the anterolateral tract. They end at the preganglionic sudorisecretory neurons and run right next to the other sympathetic fibers. Although the sympathetic system is represented in various locations of the brain, the hypothalamus is considered to be the controlling entity of all vegetative functions. This includes sweat secretion and vasomotor activity. However, the central innervation of sweat gland activity is not limited to the hypothalamus. There are several centers, which are located in different levels of the central nervous system and partly independent of one another. The cortex, the basal ganglia, diencephalic structures such as thalamus and hypothalamus, the limbic system and brain stem areas are considered possible origins of sympathetic activity (Boucsein, 2013).

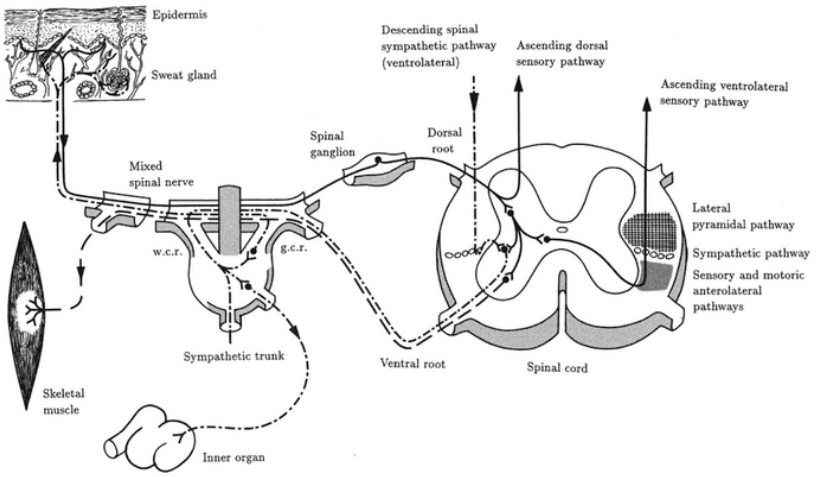

Figure 1.5: Skin afferents and efferents at spinal cord level and connections with ascending and descending pathways. —: motoric pathway, -.-: sympathetic efferents. [1]

Physiology underlying electrodermal activity

Studies, measuring sympathetic action potentials in peripheral nerves while simultaneously recording EDA, have shown a high correlation between bursts of sympathetic nerve

activity and the phasic skin conductance response (Wallin, 1981 in Cacioppo et al., 2007). Because there are many excitatory and inhibitory influences on the sympathetic system, located in various parts of the brain, there also are a variety of neural mechanisms and pathways involved into the central control of EDA. In a review on CNS elicitation of EDA, Boucsein (2013) concludes that there are two different origins above reticular level, which were already suggested by Edelberg (1972): a limbic-hypothalamatic source, which is also thermoregulatory and emotionally influenced, and a premotor-basal ganglia source, eliciting electrodermal concomitants of the preparation of specific motor actions. In addition, Boucsein suggests a third reticular modulating system, mediating EDA changes appearing with variations of general arousal (see figure 1.6). Further, an inhibitory EDA system has been located in the bulbar level of the reticular formation.

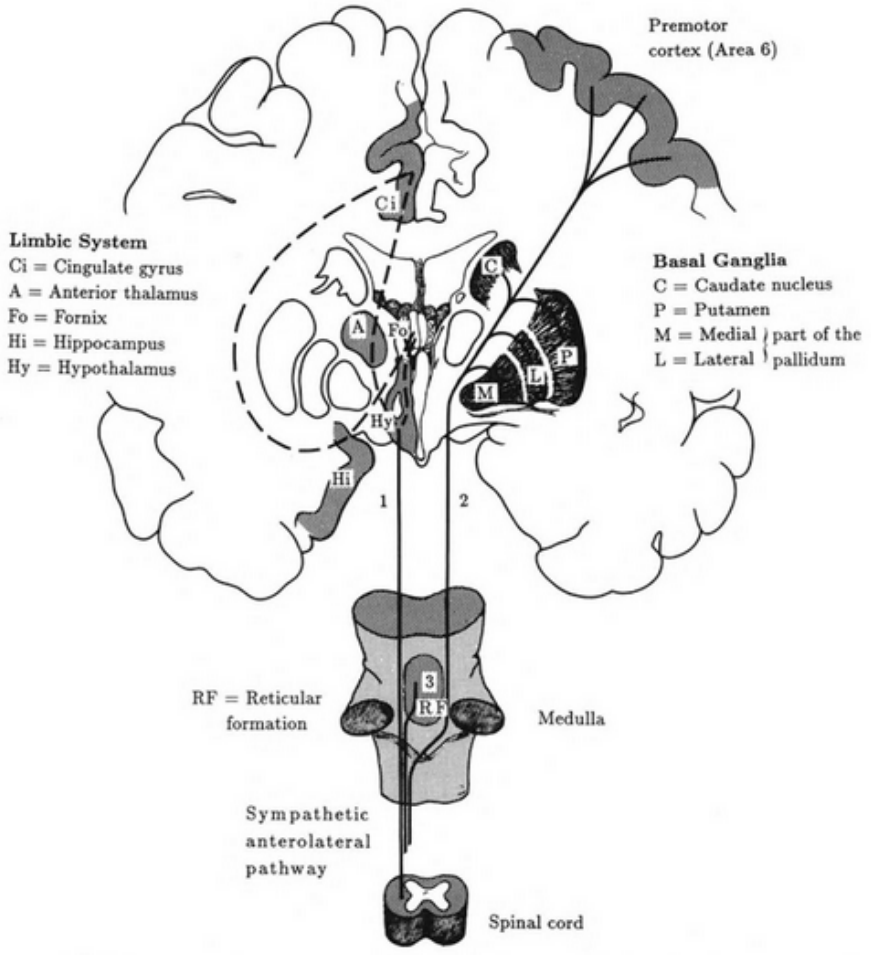

Figure 1.6: Central elicitation of EDA in humans. 1: Ipsilateral influences from the limbic system via hypothalamic thermoregulatory areas; 2: Contralateral influences from premotor cortical and basal ganglia areas; 3: Reticular influences. Dashed: Connections within the limbic system.[1]

However, there are also properties of the skin, influencing the EDA, which have to be considered, especially local physiological phenomena related to sweat gland activity. Con-

sidering the vertical structure of the skin, there is a significant difference in conductivity. Both the dermis and the subcutis are tissues with strong blood supply and interstitial fluid. Therefore their elictrical conductivity is much higher than the conductivity of the epidermal layer, which forms a diffusional as well as an electrical barrier. There has been some discussion concerning the exact localization of an epidermal diffusional barrier, which has been reviewed in detail by Fowles (1986)(Boucsein, 2013). However, most of the findings suggest that the entire stratum corneum is forming the barrier, with the exception of its desquamating surface cells(Jarret,1980, cited by Boucsein, 2013). It is to mention that, under normal physiological conditions, the skin temperature is causing changes in permeability of the skin. Fowles (1986) pointed out that the permeability for water doubles with an increase in skin temperature of 7-8 $^{\circ}C$ within the range of 25-39 $^{\circ}C$. In spite of the diffusional barrier and without activity of the sweat glands, there is always a continuous transmission of water in the skin, directed from the dermis to the outside of the body. This causes the corneum to be always partially hydrated. However, there is a distinct relationship between the relative humidity of the air and the corneal hydration. Thiele (1981) also showed a dependency of corneal thickness on the relative humidity of the air. As mentioned above there are differences in conductivity in the different skin layers. The barrier, formed by the outer epidermal layers, is penetrated by the sweat gland ducts, which act as diffusional and electrical shunts. Other than these properties, concerning the resistance, living tissue has capacitative features which are related to the activity of its membranes. While tissue conductivity is mainly responsible for tonic EDA and, in small parts, contributes to phasic electrodermal phenomena with rather slow recovery, active membrane processes following a nerve impulse are prone to eliciting electrodermal responses with fast recovery (Boucsein, 2013).

Principles of Electrodermal Measurement

There are three different methods of measuring EDA: the endosomatic method, which does not rely on the application of an external current, and two exosomatic methods, which apply either direct current or alternating current. For the past couple of decades the measurement of EDA as skin conductance, using a direct current, constant voltage methodology with silver-silver chloride (Ag/AgCL) electrodes and an electrolyte of sodium or potassium chloride has been the most prevalent method in EDA literature (Boucsein et al., 2012). Thus, the present section will focus on this method. Typically, a small voltage (e.g., 0.5V) is applied to two electrodes, which are placed on the sound surface of the skin, and a small resistor (e.g., 200 to 1000 Ω) is connected in series with the skin. To avoid any electrocardiogram artifacts, the electrodes should be placed on the same body side. Because the skin resistance exceeds the resistance of the resistor by far, its effect on the current flow inside the circuit can be neglected, when measuring the current flow. Hence, when applying Ohm's law, the current (I) flow between the electrodes, and therefore through the resistor, is equal to the voltage (U) divided by the Resistance of the skin (R_p).

$$I = U/R_p \tag{1.1}$$

Because the voltage has a constant value, the current changes in proportion to the reciprocal of the resistance, which is called conductance (G_p).

$$I \approx 1/R_p \tag{1.2}$$

Consequently, the conductance is proportional to the current flow through the skin.

$$I = U \cdot G_p \tag{1.3}$$

The unit of conductance is siemens (S), where 1 $S = 1/1\ \Omega$. According to the skin resistance usually being in the orders of $k\Omega$ or $M\Omega$, the conductance is very small and often measured in units of μS. Because the value of the series resistor (R_s) is constant, the voltage drop across R_s is proportional to the current flow I.

$$U = I \cdot R_s \tag{1.4}$$

Considering, the proportionality of I and G_p, as shown in 1.3 it becomes clear that changes in U can be monitored to provide precise index of variations in the skin conductance.

Techniques of Electrodermal Recording

This section will give a brief overview on possible requirements for electrodermal recording, such as special electrodes, electrode gels and recording devices.

Electrodes

Electrodes are a biomedical sensor system. Electrodermal recording typically relies on metal electrodes. However, metal being a generic term, as it is corroded at the surface of the electrode. Different metals will cause different stages of corrosion. Therefore, when measuring EDA with a direct current ,it is of great importance to use two electrodes of the same material, eliminating eventual potential differences. In exosomatic recording, using a direct current, the electrode pair is connected to an external voltage. Thus, turning them into anode and cathode in an electric system, which are polarized by electrolysis. The standard electrodes, used in electrodermal recording, are sintered

silver-silver chloride (Ag/AgCL) electrodes, which minimize both the polarization of the electrode and the bias potential between the electrodes. The most common form of EDA electrodes consist of a metal ring, which is embedded in a cylindrical plastic case. The space between metal and skin is filled with an electrode gel, which usually contains a chloride salt like NaCl. The concentrations of the electrode gel is chosen in the range of 0.050-0.075 molar to resemble the NaCl concentration in human sweat. Therefore, the concentration of the gel will remain stable when mixed with sweat. When using an electrolyte, it is recommended to fix the electrodes to the skin at least 5-10 minutes before starting the recording. This will eliminate an initial baseline drift in the EDA recording, caused by the electrolyte penetrating the stratum corneum and the sweat ducts. Further the electrode-skin impedance is greatly influenced by the size of the electrolyte-skin contact area and not the size of the electrode metal (Grimnes and Martinsen, 2008, p.270, cited by Boucsein et al.,2012). Therefore it is important to give special attention to the electrode fixation, guaranteeing a sufficient electrode-skin contact and a minimization of movement artifacts.

Recording Sites

Psychophysiological recordings rely on nonthermoregulatory electrodermal phenomena, which can be most reliably recorded from glabrous skin. Thus making the palms of the hands and the soles of the feet the preferred recording sites for EDA. There are three different ways to place the electrodes when recording EDA on the hand (see Figure 1.7).

It is suggested to place electrodes on the palm of the nondominant hand, presuming it is not as likely to have horny skin. In addition, the placement method # 2 should be preferred over method # 1 because of the greater responsivity (Scerbo, Freedman, Raine, Dawson and Venables, 1992, cited by Boucsein et al., 2012) and the greater sweat gland activity of the distal phalanges, compared to the other placement sites(Freedman et al.,1994, cited by Boucsein et al., 2012).
If both hands are not available for recording, EDA can also be measured at the inner site of the foot , over the abductor hallucis muscle adjacent to the sole and in between the proximal phalanx of the big toe and a point directly beneath the ankle (Boucsein et al., 2012). In case of exosomatic recording, there is usually no further pretreatment of the skin needed than washing the recording site with warm water.

Signal Evaluation

The EDA signal consists of two components, the slow, tonic skin conductance level (SCL) and the faster, phasic skin conductance response (SCR), which need to be addressed

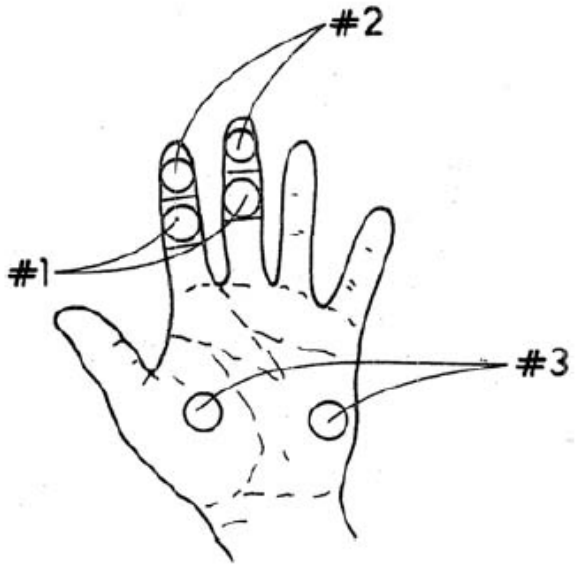

Figure 1.7: Three electrode placements for recording EDA. Placement # 1 involves volar surfaces of medial phalanges, placement # 2 involves volar surfaces of distal phalanges, and placement # 3 involves thenar and hypothenar eminences of palms.[2]

separately during the evaluation of the signal.

Phasic Electrodermal Measures

Electrodermal responses (EDRs) are short-lasting changes in EDA. They can be elicited by a distinct stimulus or occur without previous stimuli, therefore being called nonspecific EDRs (NS-EDRs). NS-EDRs are considered a tonic measure, meaning they are used to index EDA over a certain time period. In both cases the signal curve follows a certain pattern.

As shown in figure 1.8, there is a characteristic rise from the initial level to a peak, followed by a slower decline. In case of an elicited EDR the time that passes from the stimulus to the onset of the EDR is called latency (EDR lat.), which usually ranges from 1-4 seconds. As pointed out by Boucsein et al. (2012), "Latencies longer than 4 s may occur, but latencies shorter than 1 s should be treated with caution because of systemimmanent temporal delays, such as time required for processing the stimulus, autonomic nervous system nerve conduction to the sweat glands, and penetration of sweat through the ducts to the epidermis"(p. 9). Following the latency, there is an ascent time from the initial level to the peak, which typically varies between 0.5 and

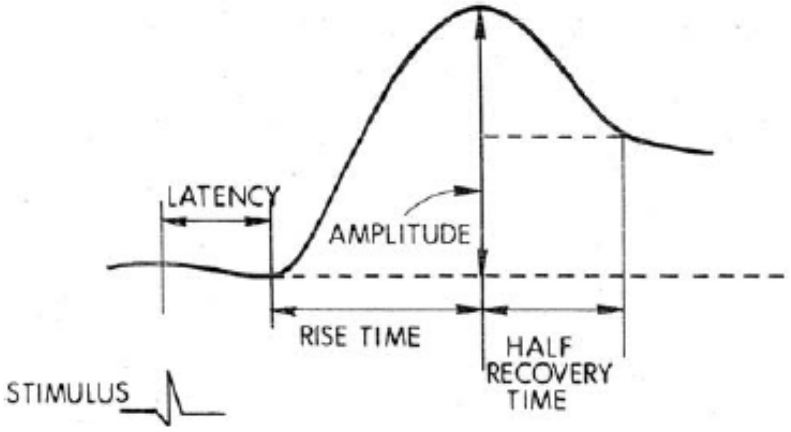

Figure 1.8: Graphical representation of principal EDA components.[2]

5 seconds (Grings, 1974, cited by Boucsein et al., 2012). The peak amplitude (EDR amp.) is reached. To determine the exact value of EDR amp., it is necessary to locate the onset point. Usually, this is done by stepping back along the SCR curve and finding the point of maximum curvature. At times it can be important to determine whether a response has occurred. The occurrence is therefore defined in terms of a minimum amplitude, that has to be reached in order for the event to be counted as a response. This is especially true for NS-EDRs. In the past the threshold value for the minimum amplitude was commonly set to 0.05 μS. Whereas nowadays, with computerized scoring of EDR records, the definition of the minimum amplitudes has been set as low as 0.01 μS. It is important to keep in mind, that choosing such a low value might lead to equipment related noise being scored as a response. After the peak deflection, the recovery begins. In this phase the electrodermal reading declines. The recovery is a much slower process than the rise. This is caused by the increase in conductivity of the corneum, elicited by sweat, in the time period following EDRs. There are certain way points, which are usually determined, e.g. the half time recovery (EDR rec.t/2), which is the time that passes until half of the amplitude has recovered. As the recovery proceeds the EDR is concluded.

Tonic Electrodermal Measures

The measures of the relatively long-term tonic EDA states can be divided into two basic principles, the skin conductance level (SCL) and nonspecific skin conductance responses (NS-SCRs). SCL refers to the level of conductance in the absence of phasic SCRs. To guarantee a distortion-free measurement of SCL, all event and artifact related SCRs have to be detected and removed. SCL is typically expressed in units of microsiemens and computed as a mean of several measurements, taken during specific time periods.

NS-SCRs on the other hand are phasic increases in skin conductance that resemble the elicited SCRs. However, they are considered to be tonic components of the EDA signal. The reasoning behind this is the absence of a distinct stimulus, related to their occurrence. According to SCL, NS-SCRs can be recording in periods without or in between a stimulus presentation, e.g. a resting phase. NS-SCRs usually are expressed in number of responses per time interval, most commonly per minute. As mentioned before it is important to define a threshold to determine which responses will be rated as such.

Psychological and Social Context of EDA

This section is based on a review of the psychological an social factors that have been shown to influence EDA, done by Cacioppo et al. (2007). Three different types of paradigm have been reviewed: (1) those that involve the presentation of discrete stimuli, (2) those that involve the presentation of continuous stimuli, and (3) those that involve examining the correlates of individual differences in EDA. The present section will briefly cover the first two types.

Effects of discrete stimuli. There are a number of stimuli attributes to which the SCR is sensitive, including stimulus novelty, arousal content, significance, intensity and surprise. Although it may be impossible to identify an isolated SCR as an "attentional" response or an "anxiety" response, it is however possible, to interpret the psychological meaning of a SCR by providing a strict experimental paradigm. The better controlled the experimental paradigm, the more conclusive the interpretation. If there is only one attribute of the stimuli changing during the experiment, such as intensity, elicited SCRs can be matched more precisely and therefor allow a better interpretation of the psychological process involved. For example, the International Affective Picture System (IAPS), which has been developed by Lang et al. (1998), consists of a variety of pictures that are rated for both their arousal-producing quality and their valence. The valence scale ranges from strongly positive to strongly negative pictures. SCRs elicited by the use of the IAPS have been found to be related to the arousal dimension, with responses increasing in magnitude as arousal rating increased for both positively valenced and negatively valenced pictures(Lang et al.,1993 , cited by Cacioppo et al.,2007).

Effects of continuous stimuli. In contrast to the brief, discrete stimuli, as reviewed earlier, continuous stimuli are rather long-lasting and can be thought of as modulating changes in tonic arousal. In this context SCL and the frequency of NS-SCRs provide the most useful measures of EDA, because they can be measured over long periods of time. There are certain continuous stimulus situation which will reliably produce an increase in EDA. One example that can be mentioned here is performing a task. Performing as well as anticipating almost any task will cause an increase of both SCL and the NS-SCR frequency. This has already been shown by different studies. Lacey et al.

(1963) recorded palmar SCL during rest and during anticipation and performance of eight different tasks. They confirmed an increase of SCL in every task situation. According to the results the SCL rose by one μS during anticipation and by another one or two μS during performance, when compared to the resting level. Other findings suggest that situations in which strong emotions are elicited also increase tonic EDA arousal. Ax(1953) created genuine states of fear and anger in his subjects by causing them to believe to feel in danger of a high-voltage shock due to equipment malfunction or by treating them in a rude fashion. Both SCL and NS-SCRs rose during the fear as well as the anger conditions (Cacioppo et al., 2007).

In conclusion, EDA is a sensitive peripheral index of sympathetic nervous system activity. As mentioned above, the eccrine sweat glands are entirely under sympathetic control and therefore increases in both SCL and SCR mirror tonic and phasic sympathetic activation. EDA provides for a relatively direct and inexpensive measure that comes with great utility and can be used as an reliable indicator of arousal and attention.

1.1.4 Electrocardiogram

Anatomical and Physiological Basis

The cardiovascular system consists of two main components, the heart, which functions as a pump, and the vasculature, as a distribution system, that together ensure a constant blood supply throughout the whole body. The heart provides a steady flow of oxygenated blood, by sending blood into the lungs (pulmonary circulation) and then to the rest of the body (systemic circulation).

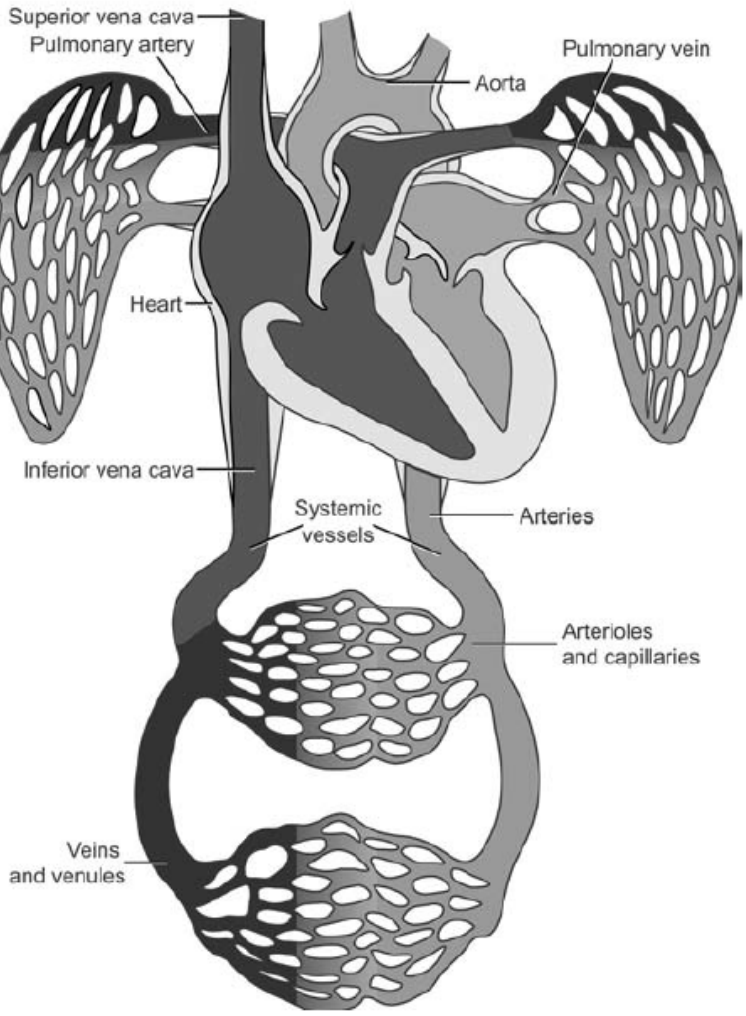

Figure 1.9: Ventral perspective of the systemic and pulmonary circulation.Lighter gray areas indicate oxygenated blood and darker gray areas indicate deoxygenated blood.[2]

As can be seen on figure 1.9 the deoxygenated blood returns to the heart through the

superior and inferior vena cava. After passing the right atrium the venous blood reaches the right ventricle of the heart, from where it is pumped into the lungs for re-oxygenation purposes. Completing the pulmonary circulation, the oxygenated blood returns to the heart through pulmonary veins, reaching the left atrium first and finally the left ventricle. From here the blood is pumped into the aorta and distributed in the rest of the body. On its way to the periphery the blood passes through ever smaller vessels, starting with large arteries, which later branch into smaller arterioles and finally into capillaries. The capillaries are small, thin walled vessels from which oxygen, nutrients and waste products, such as carbon dioxide, are exchanged with the tissue. Leaving the capillaries, the blood returns to the heart again through the venous part of the systemic circulation. After passing the slightly larger venules the blood flows into increasingly larger veins until it reaches the vena cava and the circle closes.

The human heart can be divided into four chambers, two on either side. Each of the sides consists of an atrium at the top, or rostral, half and a ventricle at the bottom, or caudal, half. The heart contains three different types of cardiac muscle tissue, atrial and ventricular muscle fibers as well as specialized conducting fibers. The muscle fibers primarily serve the pumping function of the heart but also form a syncytium. This means, the tissue is electrically coupled in a way that allows for a rapid spread of depolarization along the longitudinal axis of the heart. There are two separate syncytiums, the atrial and the ventricular one, which are connected by an electrical conducting system. Although they are electrically connected it is crucial that both portions of the heart function as separate pumping units and all chambers are coordinated, in a way where the ventricular action is always triggered shortly after the atrial action.
This challenge is met by a special conducting system, formed out of specialized conducting fibers, which is embedded into the cardiac muscle tissue. The contraction of the heart can be triggered by the depolarization of two nodes of electrically active tissue, the first one being the sinoatrial (SA) node followed by the atrioventricular (AV) node. The SA node, serves as the pacemaker of the heart and is located inside the wall of the right atrium right beneath the entering point of the vena cava superior. A system of internodal, conductive fibers connects the two nodes. The depolarization wave is transported into the ventricles by passing the bundle of His, which branches into the left and right bundles and then transition into the Purkinje fibers. These fibers pass through the interventricular septum and deliver the depolarization into the rest of the ventricles.
The cardiac cycle is a term that describes all events that occur in the heart from one beat to the next (see figure 1.11). The cycle is divided into two main phases, the diastole and systole. During the systole the pumps and the blood is evacuated into the arteries, whereas the heart will be filled again during the diastole. The electrocardiogram (ECG) is the graphical representation of the electrical potential produced by the electrical current passing through the heart. It is recorded via electrodes positioned on the body surface and displayed in forms of so called waves or deflections (Abdullah, 2014).

The cycle starts with the depolarization of the SA node during the final stage of the

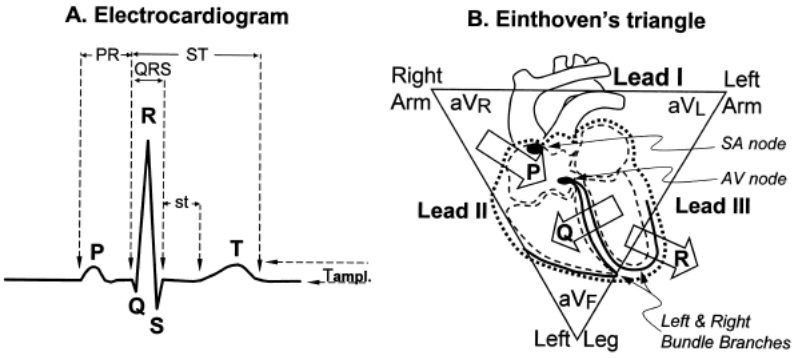

Figure 1.10: A: General morphology of the ECG showing P, Q, R, S, and T components, the PR, ST and QRS intervals, the st segment, and the T wave amplitude; B: The heart, conducting system, and Einthoven's triangle. Open arrows indicate thedirection of propagation of electrical activation and the associated component of the ECG.[2]

diastole. The process of the depolarization wave passing through the atrial muscle tissue corresponds to the P wave of the ECG. Following the P wave is the atrial contraction, during which the QRS complex appears in the ECG. This complex reflects the contraction of the ventricles and the demarcation of the onset of the systole. During the contraction, the intraventricular pressure reaches levels high enough to close the AV valves, which are located between the atria and the ventricles. After the ventricular contraction has ended the ventricular pressure will start to drop again, eventually causing it to fall below the atrial pressure and allowing the AV valves to open and the blood to fill the ventricles. However, once the the ventricular pressure exceeds the aortic pressure the aortic valve opens and blood is evacuated into the systemic circulation. In the latter part of the ventricular contraction phase the ventricles repolarize, creating the T wave in the ECG and initiating the relaxation of the ventricles as well as the onset of diastole.

ECG Measurement

As mentioned above, the ECG is a graph that represents cardiac electrical activity from one instant to another. The ECG pictures the heartbeat in the form of a time-voltage chart. The general study of ECGs, including its clinical applications and technological aspects, is called electrocardiography (Goldberger et al., 2017). Accordingly, the device, used to measure and display the conventional (12-lead) ECG, is called an electrocardiograph. It records the cardiac electrical activity through electrodes, which are positioned selectively on the body surface. Current ECGs most commonly use disposable self-adhesive silver-silver chloride electrodes, which were traditionally placed on the limbs. These extremity leads can be represented by the Einthoven triangle (see Figure 1.10B). As illustrated

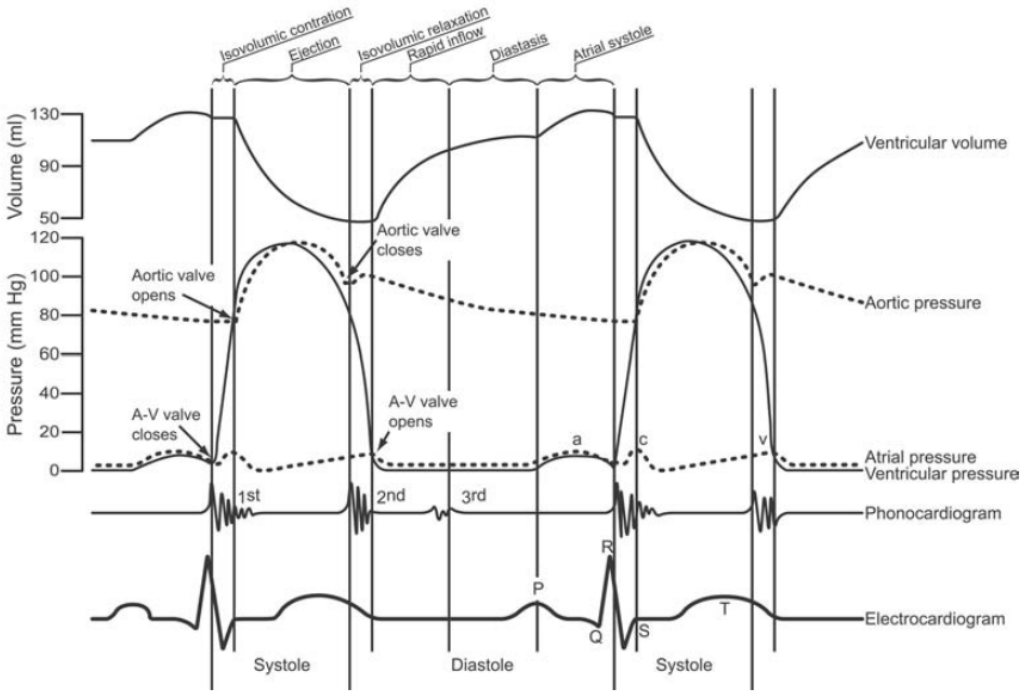

Figure 1.11: The graphic shows two full cardiac cylces for various aspects, which can be seen on the right.[2]

there are six leads in total, three unipolar leads, which are taken of the right arm (aV_R), the left arm (aV_L) and the left leg (aV_F), as well as three bipolar leads, taken between I: left arm - right arm, II: left leg - right arm and III: left leg -left arm, with the right leg being the ground. Typically these leads are approximated by placing the electrodes on the torso instead of the limbs. In clinical cardiology, a series of unipolar precordial chest leads are usually added to provide a variety of distinct electrical perspectives on certain heart events. These leads start from the right lower peristernal region, with the first lead being labeled V1, and extend laterally to the left (V2-V6). However, for most psychophysiological applications a simpler configuration, such as lead II, will suffice as they still yield a large enough R wave (Cacioppo et al., 2007).

ECG Signal components

The present section is based on the work of Goldberger et al. (2017) and will briefly outline all components of an ECG signal. The clinical ECG graph consists of three different component types, waveforms, intervals and segments. Their distribution is specified by the 5-4-3 rule, which states that there are five waveforms (P, QRS, ST, T and U), four sets of intervals (PR, QRS, QT/QTc and RR/PP) and three segments (PR,

ST and TP)(Goldberger et al., 2017).

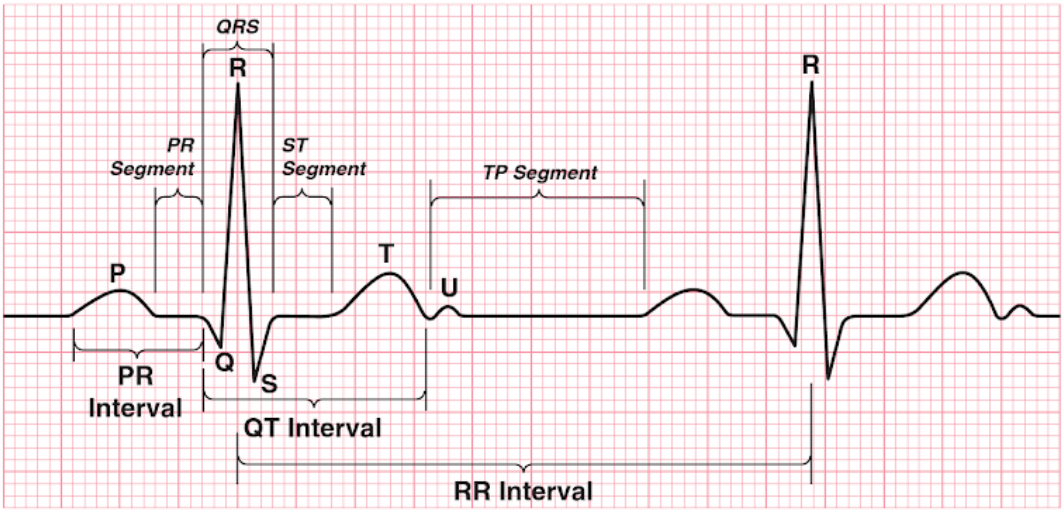

Figure 1.12: Summary of all major components of the ECG graph. Note that ST can be considered as both a waveform and a segment.[3]

Waveforms. The five basic ECG waveforms are named alphabetically, starting with the P wave, which represents atrial depolarization. The QRS waveform, which is often referred to as QRS complex, represents the ventricular depolarization. The ST and T wave represent the ventricular repolarization, eventually resulting in the U wave depicting the final stage of said repolarization. The atrial repolarization is generally not observed, because of the small amplitudes of the atrial ST segment and atrial T wave. Together these waveforms represent a complete cycle of the electrical activity of the heartbeat.

Segments. As mentioned before there are three basic segments contained in the ECG graph, which are defined as the spaces between two waveforms. The PR segment is defined as the distance between the end of the P wave and the start of the QRS complex. It marks the start of atrial repolarization, which is continued throughout the QRS complex and ending during the ST segment. The ST segment spreads from the end of the QRS complex to the beginning of the T wave. TP segment connects the end of the T wave with the beginning of the P wave of the next cycle. This segment represents the electrical resting state and is typically used as a baseline reference for PR and ST deviation assessment in clinical diagnostics.

Intervals. Per definition intervals are parts of the ECG that include a minimum of one entire waveform. The PR interval is measured from the beginning of the P wave to the beginning of the QRS complex and is followed by the QRS interval, which lasts until the end of the same QRS complex. The QT interval is defined from the start of the QRS complex to the end of the T wave. The RR interval is the last of the four and lasts for

an entire heart cycle, starting and ending at a predefined point in the QRS complex, which is often referred to as the R point. It can be used to calculate the instantaneous heart rate (HRi) in the following manor.

$$HRi = 60/RR \qquad \text{,RR in units of seconds} \tag{1.5}$$

Psychophysiological Measurements

Heart rate and heart period. The heart period (HP) is the time in milliseconds between two heart beats. It is usually determined by measuring the distance between to successive R spikes in an ECG, due to their prominence in comparison to the other components. The heart rate (HR) is a more common way when communicating heart activity. Typically the heart rate is given in beats per minute (bpm) and can be determined by calculating the reciprocal of the heart period.

$$HR = 60000/HP \tag{1.6}$$

There are incidents however, in which heart rate and period are not linear. As mentioned by Caciappo et al. (2007) "Berntson and colleagues (1995) reviewed literature across several mammalian species, including humans, showing that the relationship between changes in activity of the parasympathetic and sympathetic autonomic branches and heart period are more nearly linear than the relationship between activity in either branch and heart rate". This means that certain change in activation of either branch of the ANS will result in an equal change in heart period, whereas the same is not true for heart rate. It is important to mention that the change in heart period is independent from the baseline heart period at the time. For example, raising the stimulation frequency of the vagal nerve by 2 Hz in dogs, results in a change of 70-72 msec in heart period, regardless of the baseline heart period being either 875 msec or 350 msec. In contrast, applying a 2 Hz change in parasympathetic activation resulted in different heart rate changes for either baseline. Heart rate of dogs with a heart period baseline of 875 msec changed by 5.1 bpm and by 29.2 bpm for a 350 msec baseline (Parker et al. , 1984, cited by Cacioppo et al., 2007). Therefore the choice of the metric can heavily influence the outcome of an experiment. Bernston et al. (1995) recommended heart rate as the metric of choice when changes in cardiac functions are likely to be caused by autonomic effects and when those changes vary widely as a result of an experimental manipulation or between groups because errors caused by the nonlinear relationship between autonomic inputs and heart rate can be significant and result in misinterpretations of the data (Bernston et al., 1995, cited by Cacioppo et al., 2007).

Heart rate variability. The oscillation in the interval between consecutive heart beats as well as the oscillation between consecutive instantaneous heart rates is called heart rate variability (HRV)(Task Force of the European Society of Cardiology the North American Society of Pacing Electrophysiology, 1996 ; from now on Task Force). Measures of the HRV can be divided into three general groups, the time domain methods, the frequency domain methods and non-linear methods. Time based methods determine either the HR at any given point in time, by calculating the HRi, or the intervals between successive normal complexes, by detecting the so called normal-to-normal (NN) intervals. Simple time–domain variables that can be calculated include the mean NN interval, the mean heart rate and the difference between the longest and shortest NN interval(Task Force, 1996). Frequency domain methods on the other hand decompose the overall heart period variance into specifiable frequency bands(Bernston et al. 1995; Task Force, 1996, cited by Cacioppo et al., 2007). A common approach are power spectral density (PSD) analysis, which are based on a Fast Fourier Transform (FFT) of the HRV and provide basic information on how power distributes as a function of frequency. When considering only short time HRV recordings ranging from 2 to 5 minutes three major spectral components can be distinguished. There are very low frequency (VLF), low frequency (LF) and high frequency (HF) components (Task Force, 1996). The distribution of the power and the central frequency of each frequency band vary in regard to changes in autonomic modulation of the heart period. In general high-frequency HRV is mostly attributable to variations in the parasympathetic control associated with respiration and is commonly used as an index of vagal control of the heart (Cacioppo et al., 2007). Whereas low-frequency HRV's psychological significance remains a controversial topic. Contrary to the assumption of LF HRV being related to cardiac sympathetic activity it seems to rather reflect both sympathetic and vagal influences related to baroreflex mechanisms (Berntson et al., 1997).

Non-linear phenomena are determined by a number of complex interactions of haemodynamic, electrophysiological and humoral variables, as well as autonomic and central nervous regulations (Task Force, 1996). Although a variety of techniques has been applied to determine non-linear properties no major breakthrough in the field of HRV analysis has been achieved yet.

1.1.5 Exposure Therapy

1.2 General

1.2.1 State of the Art

1.2.2 Recent Advances in Research

1.3 Problem Analysis and Goals

2 Materials and Methods

2.1 Materials and Methods

All experiments and measurements were conducted within the facilities of Systems Neuroscience and Neurotechnology Unit, especially the Green Lab, which is located at the Saarland University Hospital.

2.1.1 Participants

2.1.2 System Setup

2.1.3 Virtual Reality Exposure

To display the virtual environment, a powerful computer(specs) and an Nvidia GeForce GTX 1080 (pheonix) graphics card with 8 GB of dedicated memory were used in combination with the HTC-Vive head-mounted display (HMD). The Dual AMOLED displays (3,6" diagonal) of the HMD provided for a high-resolution presentation of the virtual world, with 1080x1200 pixel on each eye. The distance between the pupils was manually adjusted for each participant by means of a knob on the HMD. The Lighthouse Tracking-System, created by the company Valve, allowed to track participant's motion during the exposure in an area of maximal 5 by 5 meter and to project their movement in the virtual environment. The Tracking-System consisted of two stationary sensors, positioned in opposing corners at a height of roughly 2 m, and all the sensors, which were attached to the HMD and the controller by HTC. The program, which was used to remotely control the virtual environment, was written with the Matlab software version R2015a. The virtual environment itself was created with Unity version 5.6.1f1 personal.

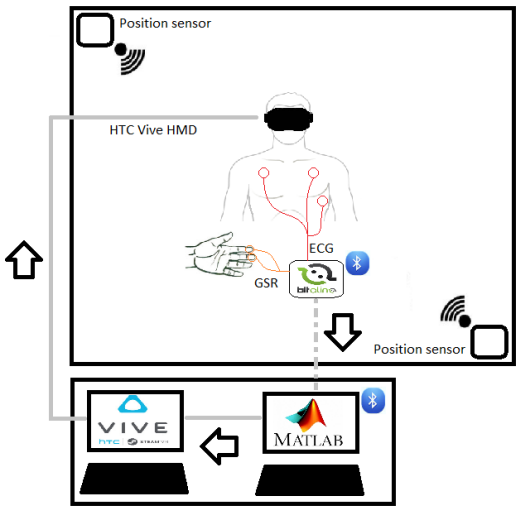

Figure 2.1: Closed-loop virtual reality system.

Therapy environment

The virtual environment was built with the Unity software ... We have designed our virtual height situation around the concept of a closed room featuring a descending floor. A design, which has been chosen specifically over different approaches that have been used in the past.

2.1.4 Procedure

- how many subjects did participate?
- which tasks did the patients fullfill? (cross the bridge etc.)
- duration of the experiment

- description of the virtual environment, the procedure (baseline measurement,VRET in detail)
- pictures that show the VE in it's starting state as well as it's therapy state (descended floor)
- description of how the VR is controlled by the user(which parameters can be influenced)

- main objective is the measurement of gsr during the therapy and the evaluation of the gsr data concerning the stress of the patient during the therapy
- how is the gsr information processed and evaluated?
how is it presented to the user?
- description of how the VR is controlled by the user(which parameters can be influenced)
- graphic of control chain

-ECG processing frequency domain methods PSD (in task force , reason which method to pick)

3 Results

4 Discussion

5 Conclusions and Future Work

A Tables and Measurement Results

List of Figures

List of Tables

Bibliography

[1] W. Boucsein. *Electrodermal Activity*. The Springer Series in Behavioral Psychophysiology and Medicine. Springer US, 2013. ISBN 9781475750935. URL https://books.google.de/books?id=0hXrBwAAQBAJ.

[2] J.T. Cacioppo, L.G. Tassinary, and G.G Berntson. *Handbook of Psychophysiology*. Cambridge University Press, 2007.

[3] A.L. Goldberger, Z.D. Goldberger, and A. Shvilkin. *Clinical Electrocardiography: A Simplified Approach E-Book*. Elsevier Health Sciences, 2017. ISBN 9780323508773. URL https://books.google.de/books?id=q59tDgAAQBAJ.